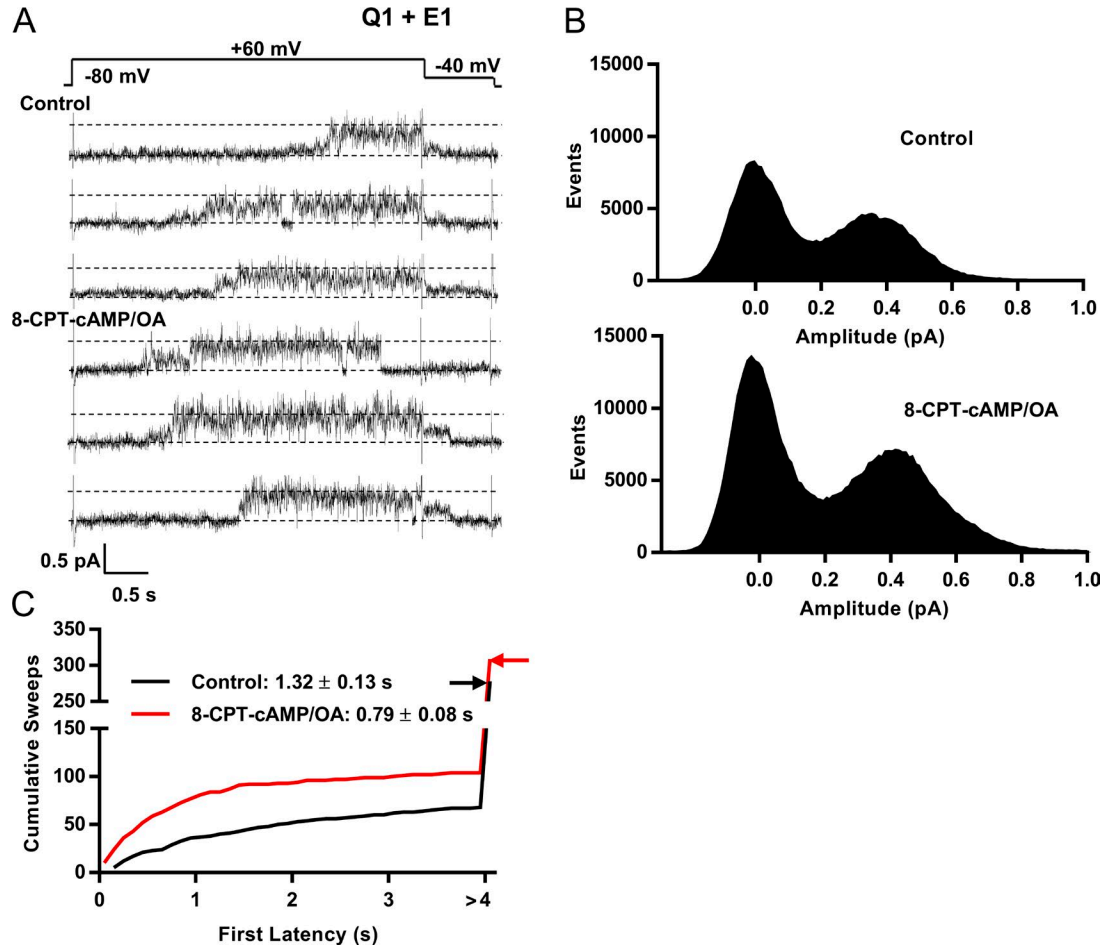Figure S1. **Effects of cAMP on first latency and amplitude of Q1 and E1 separately expressed with Yotiao.** (A) Single-channel sweeps of Q1+E1 expressed with Yotiao in control (top) and after addition of 200 µM 8-CPT-cAMP/0.2 µM OA (bottom three sweeps). (B) All-points histograms of active control sweeps (top, cumulated from eight sweeps) and active sweeps during cAMP exposure (bottom, cumulated from 14 sweeps). (C) Cumulative latency histogram. Mean first latency for the 68 active control sweeps of 278 was 1.32 ± 0.13 s. With 200 µM 8-CPT-cAMP/0.2 µM OA, mean first latency for the 104 active sweeps of 309 was 0.79 ± 0.08 s; P = 0.0002 (see Table 1). Sweeps without activity were given a first latency >4 s. Note split-scale ordinate.

The Journal of General Physiology

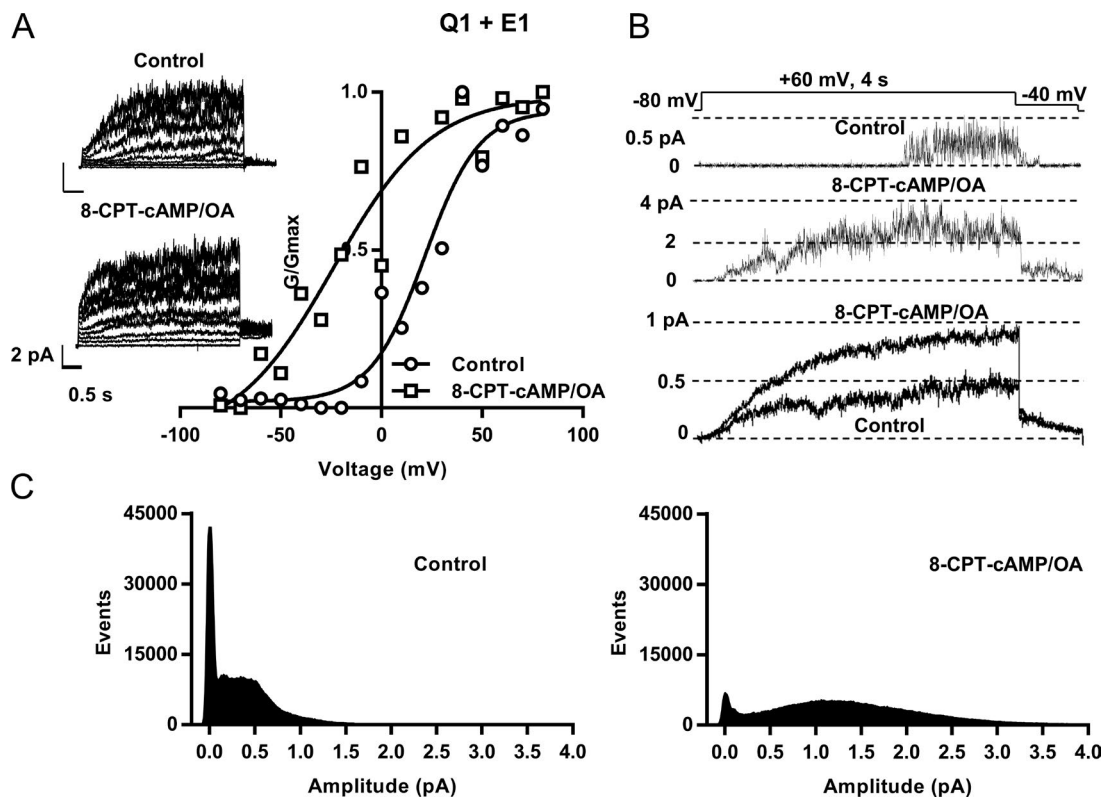JGP   cAMP effects on I_{Ks} gating | Thompson et al.   S19

Figure S2. **8-CPT-cAMP increases the number of active channels and causes a hyperpolarizing shift of the $V_{1/2}$ with Q1+E1.** (A) G-V curves from a macropatch before and after 8-CPT-cAMP exposure. Control (circles, $V_{1/2}$ = 21.6 mV), 8-CPT-cAMP (squares, $V_{1/2}$ = −23.9 mV). Inset shows macropatch currents in control and with 8-CPT-cAMP. Cells were held at −80 mV and pulsed from −60 mV to 80 mV in 10-mV steps (every other trace is shown). Tails were recorded at −40 mV for 900 ms. (B) Sample single-channel sweep from I_{Ks} plus Yotiao-expressing patch (control) and after adding 8-CPT-cAMP/OA. Bottom, ensemble average of 24 sweeps before and after 8-CPT-cAMP/OA addition. (C) All-points histograms of active sweeps in control (left, 24 sweeps) and when exposed to 8-CPT-cAMP (right, 24 sweeps).
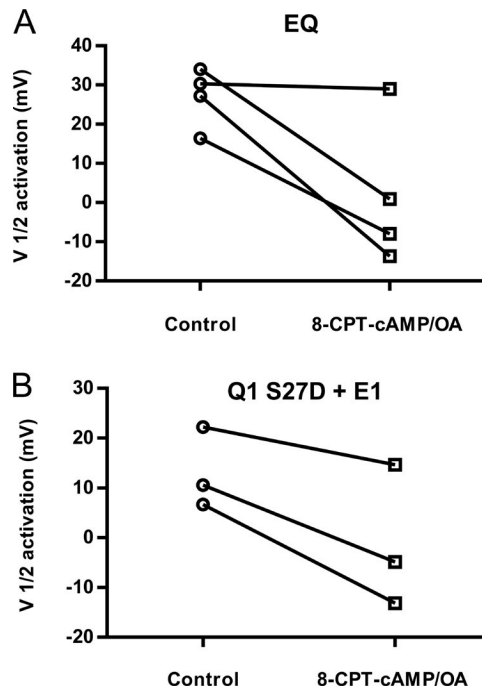
Figure S3.   Effects of cAMP on V$_{1/2}$ of activation in macropatches. (A) V$_{1/2}$ of activation for EQ macropatches before (circles, mean V$_{1/2}$ = 27 ± 3.82 mV) and after (squares, mean V$_{1/2}$ = 2.07 ± 2.03 mV) 200 µM 8-CPT-cAMP/0.2 µM OA, *n* = 4. (B) V$_{1/2}$ of activation for Q1 S27D+E1 macropatches before (circles, mean V$_{1/2}$ = 13.1 ± 4.7 mV) and after (squares, mean V$_{1/2}$ = −1.13 ± 8.24 mV) 200 µM 8-CPT-cAMP/0.2 µM OA, *n* = 3.
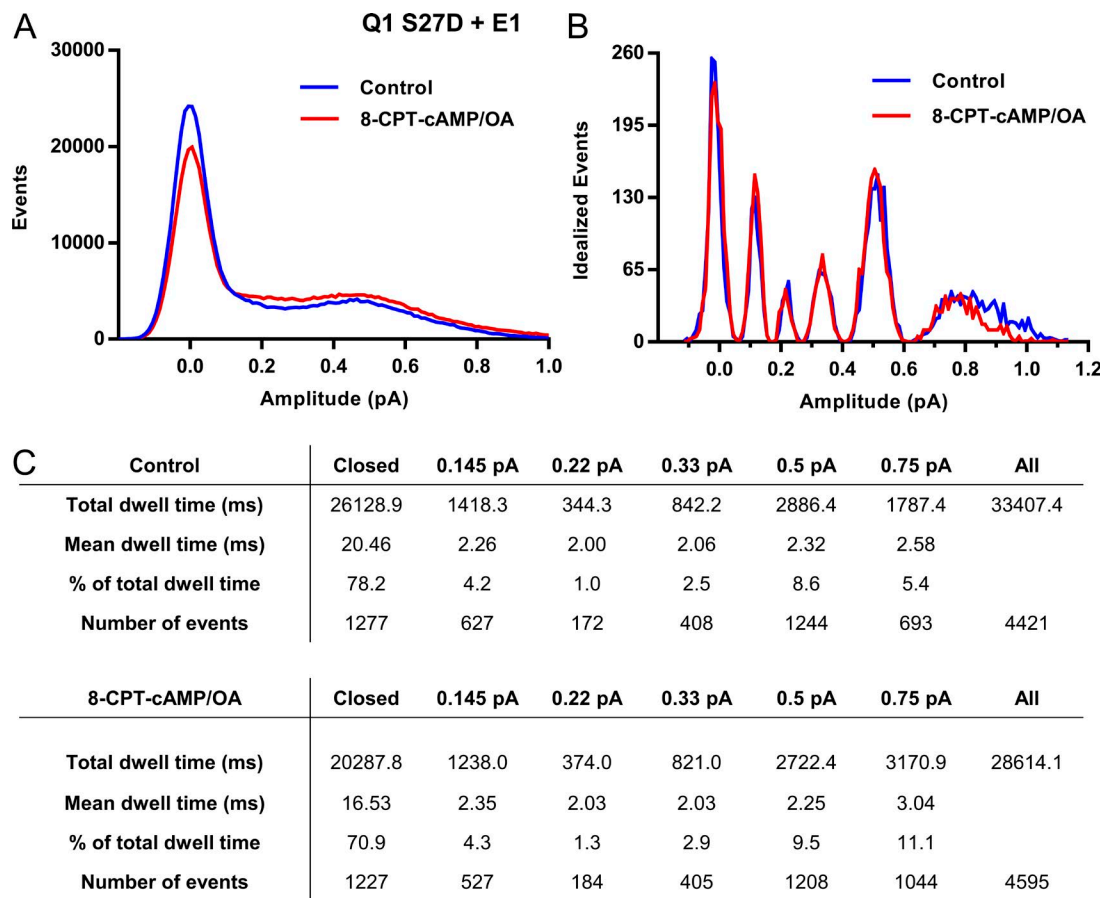
A Q1 S27D + E1

B

Figure S4. Subconductance analysis of S27D+E1 before and after 8-CPT-cAMP/OA. (A) Raw all-points histograms of 13 control sweeps (blue) from an S27D+E1 patch and after 200 µM 8-CPT-cAMP/0.2 µM OA (red). (B) Idealized histograms of 13 control sweeps (blue) and 13 8-CPT-cAMP sweeps (red). Five thresholds were used for the idealization process: 0.145, 0.22, 0.33, 0.5, and 0.75 pA. Right, also 13 sweeps, but in the presence of 8-CPT-cAMP/OA. (C) The table shows total and mean dwell times (milliseconds) for each of the different thresholds, the percentage of time spent at each level, and the number of events at each threshold before and after 8-CPT-cAMP addition. The bin width is 0.01 pA. Only events longer than 1.5 ms were used. Data were filtered at 500 Hz.
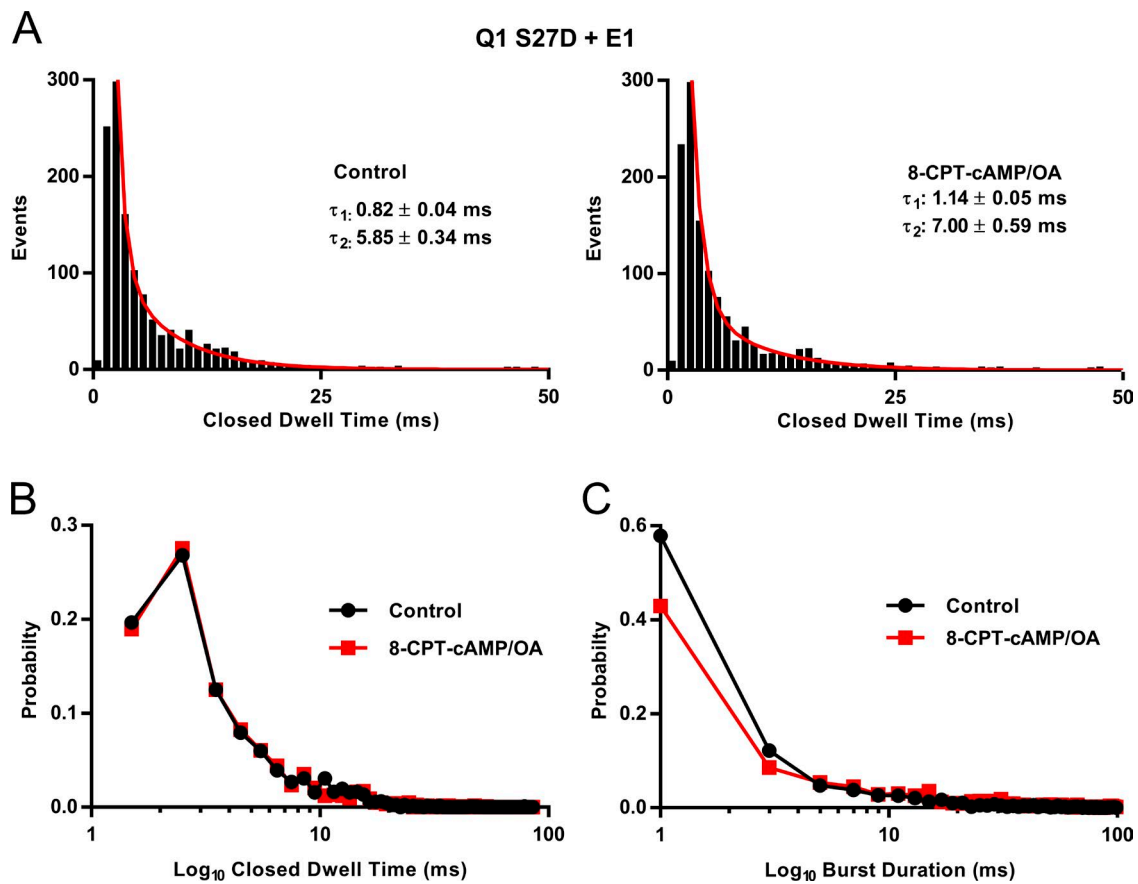
C

Control	Closed	0.145 pA	0.22 pA	0.33 pA	0.5 pA	0.75 pA	All
Total dwell time (ms)	26128.9	1418.3	344.3	842.2	2886.4	1787.4	33407.4
Mean dwell time (ms)	20.46	2.26	2.00	2.06	2.32	2.58	
% of total dwell time	78.2	4.2	1.0	2.5	8.6	5.4	
Number of events	1277	627	172	408	1244	693	4421

8-CPT-cAMP/OA	Closed	0.145 pA	0.22 pA	0.33 pA	0.5 pA	0.75 pA	All
Total dwell time (ms)	20287.8	1238.0	374.0	821.0	2722.4	3170.9	28614.1
Mean dwell time (ms)	16.53	2.35	2.03	2.03	2.25	3.04	
% of total dwell time	70.9	4.3	1.3	2.9	9.5	11.1	
Number of events	1227	527	184	405	1208	1044	4595

cAMP effects on I_{Ks} gating | Thompson et al.

Figure S5. **S27D+E1 closed dwell times and burst analysis.** (A) Closed dwell time distributions for S27D+E1 from 13 sweeps before and 13 sweeps after 200 μM 8-CPT-cAMP/0.2 μM OA, filtered at 500 Hz. The data were fitted with the sum of two exponential functions. τ_1: 0.82 ± 0.04 ms (AUC 236.61 ± 7.16) and τ_2: 5.85 ± 0.34 ms (AUC 105.79 ± 6.69) in control. After 8-CPT-cAMP/OA, τ_1: 1.14 ± 0.05 ms (AUC 258.48 ± 7.48) and τ_2: 7.00 ± 0.59 ms (AUC 71.52 ± 7.18). Bin width was 1 ms. (B) Probability distribution of closed time durations in control (black) and after 8-CPT-cAMP/OA (red), from data in A. (C) Probability distribution of burst durations in control (black) and after 8-CPT-cAMP/OA (red), from data in A. Event histograms were fitted with the sum of two exponential functions. In control τ_1: 1.26 ± 0.04 ms (AUC 663.79 ± 7.28) and τ_2: 15.55 ± 2.53 ms (AUC 43.65 ± 5.87). In 8-CPT-cAMP, τ_1: 1.23 ± 0.05 ms (AUC 452.64 ± 7.03) and τ_2: 21.04 ± 2.89 ms (AUC 47.582 ± 4.95). Bin width was 2 ms. Only events longer than 1.5 ms in duration were used in this analysis.
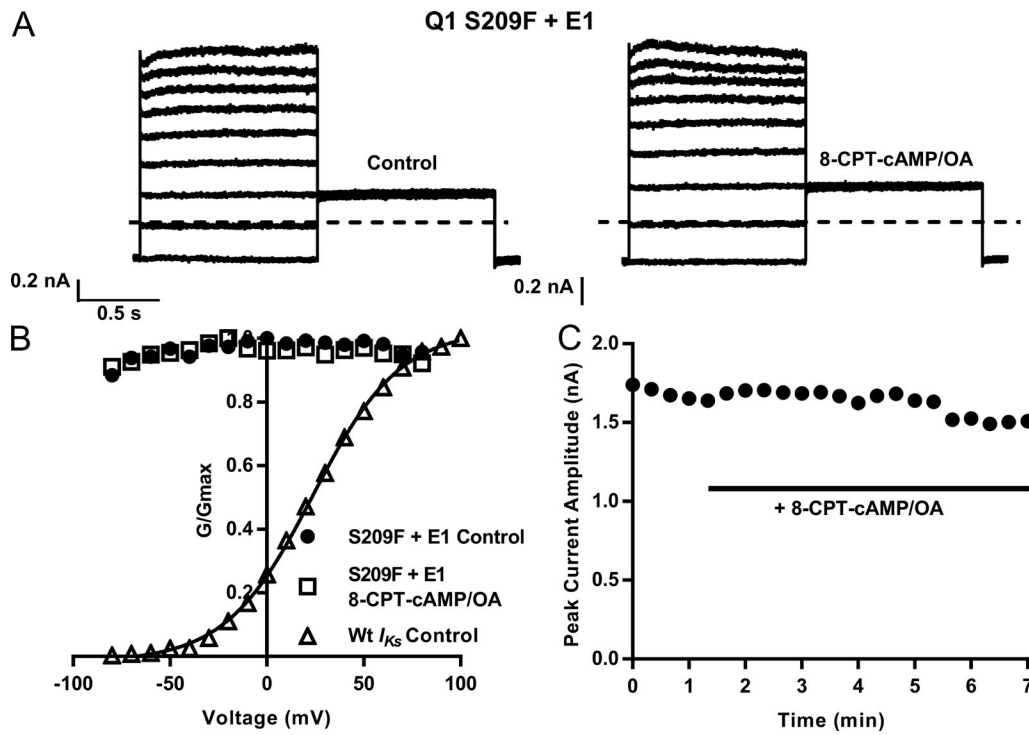
Figure S6.   **Whole-cell currents from S209F+E1 and Yotiao are unaffected by 8-CPT-cAMP.** (A) Currents from S209F+E1 before (left) and after (right) 200 µM 8-CPT-cAMP + 0.2 µM OA. The holding potential was −80 mV, and the cell was pulsed for 1 s from −80 to 80 mV in 10-mV steps. Every other current record is shown. The tail current was recorded at −40 mV for 1 s. (B) S209F+E1 G-V relationship plotted using the tail currents, data from a single cell. G-V data for WT I_{Ks} is also included ($V_{1/2}$ = 25.1 ± 2.5 mV, n = 11). (C) Diary plot of the peak S209F+E1 current at 60 mV before and after the addition of 200 µM 8-CPT-cAMP + 0.2 µM OA. Black line denotes the time at which 8-CPT-cAMP was present in the bath.

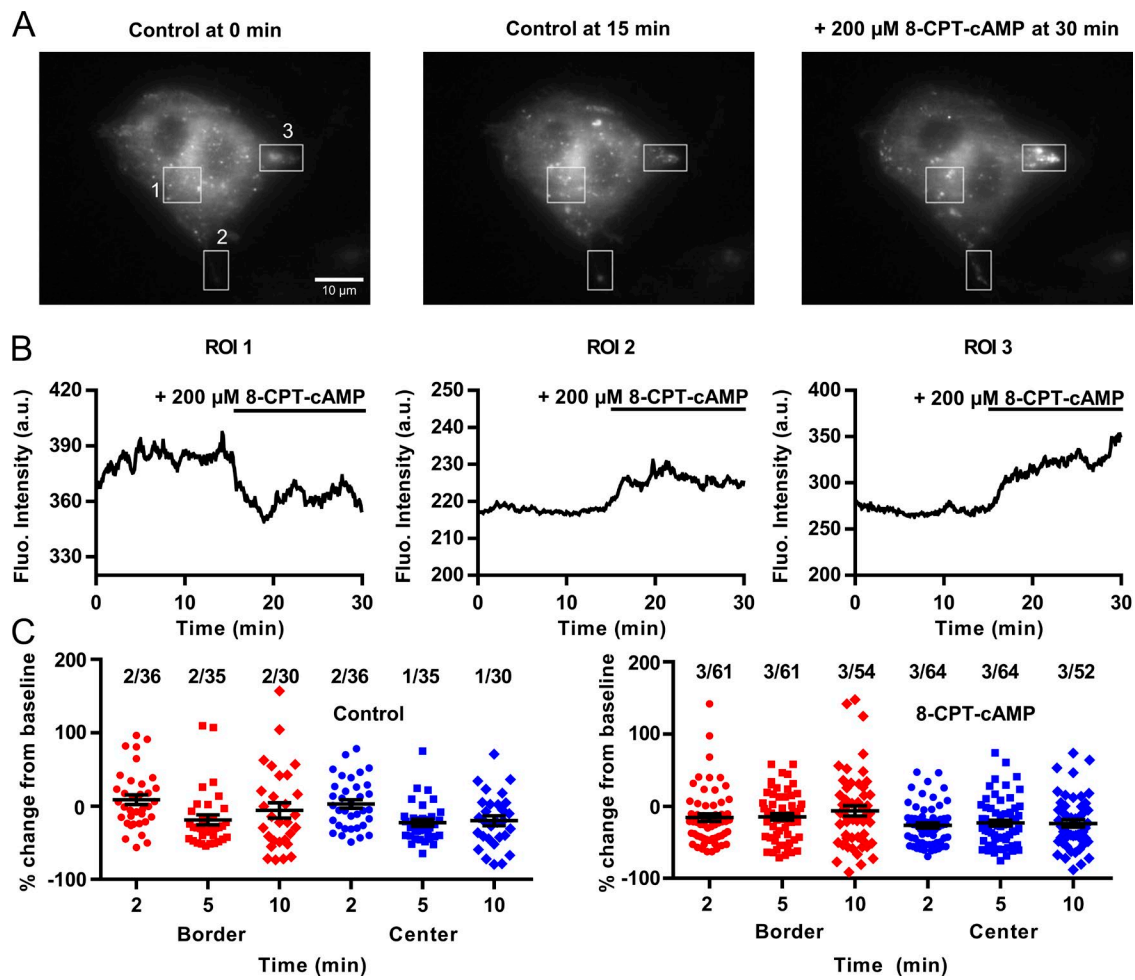cAMP effects on I_{Ks} gating | Thompson et al.

Figure S7. **KCNQ1 channels are highly mobile in CHO cells.** (A) TIRF images of KCNQ1-GFP control at 0 min (left), 15 min (middle), and 15 min after addition of 200 µM 8-CPT-cAMP at 30 min (right). (B) Diary plots representing change in fluorescence of ROI 1 (left), ROI 2 (middle), and ROI 3 (right) over time. 200 µM 8-CPT-cAMP was added at 15 min. (C) Percentage change from baseline in different ROIs after control solution (left) and 8-CPT-cAMP (right) was added to the bath. Black lines overlaying points show means ± SE of the distributions. The cell is divided into many ROIs and grouped into either the border (red) or center (blue) of the cell at three different time points: 2, 5, and 10 min after either 8-CPT-cAMP or control vehicle was added. The number of ROIs in each group and time point is shown. Above the figure are the number of ROIs in which a significant change in fluorescence was seen, relative to the total number of ROIs observed.
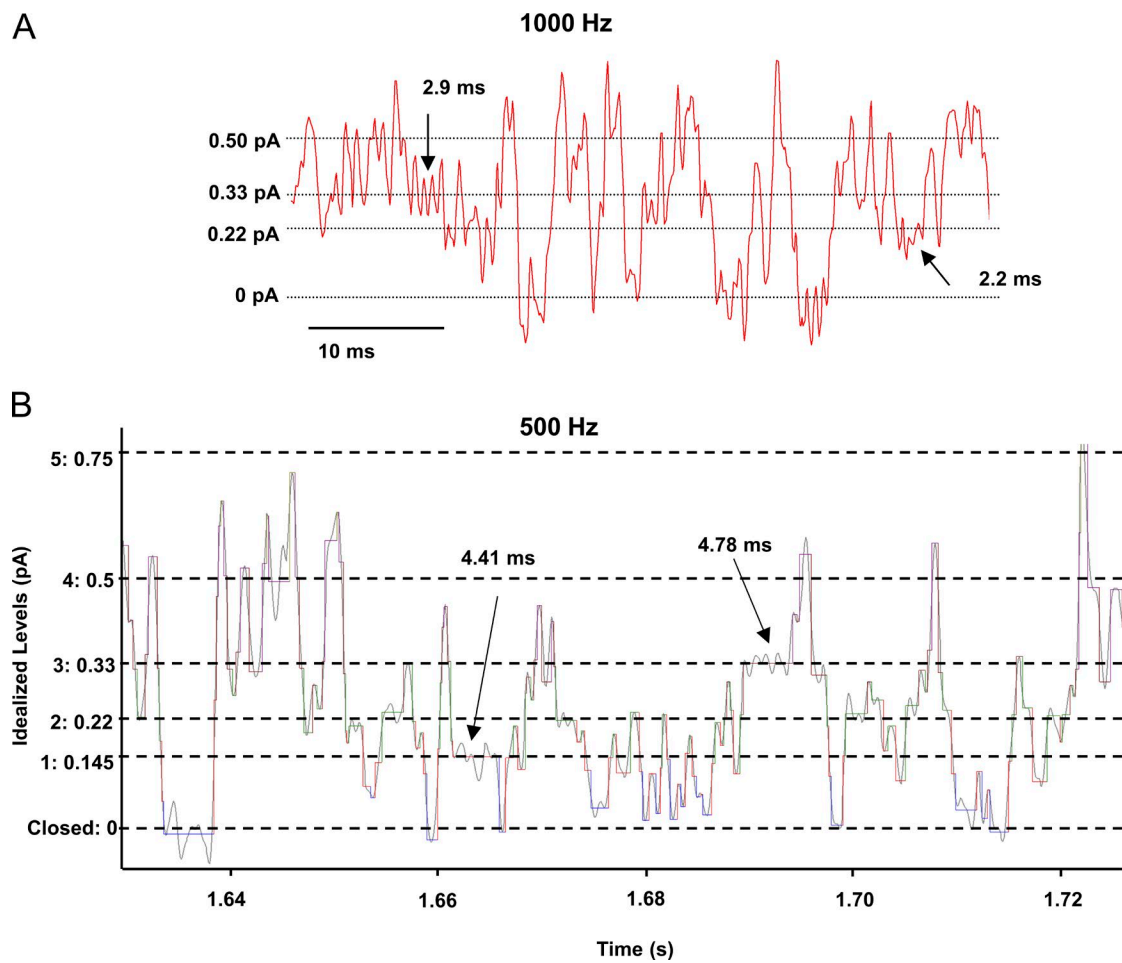
Figure S8. **Example of idealization of a single-channel current trace in Clampfit 10.5.** (A) Scaled version of a KCNQ1 + KCNE1 single-channel recording filtered at 1000 Hz, highlighting two >2-ms subconductance events (arrows). (B) Section of an EQ single-channel current record during a step to 60 mV over a period of 95 ms. The data were filtered at 500 Hz after acquisition at 2 kHz (red line). Dashed lines indicate the five conductance levels (0.145–0.75 pA) as well as the closed level. The idealized events are color coded by level (closed is blue, level 1 is red, level 2 is green, level 3 is maroon, level 4 is purple, and level 5 is tan). Two subconductance events are highlighted as having durations of >4 ms (identified by arrows), a level 1 and a level 3 event.

cAMP effects on I_{Ks} gating | Thompson et al.